MIT Libraries | DSpace@MIT

MIT Open Access Articles

Fatigue exhaustion of the mitral valve tissue

The MIT Faculty has made this article openly available. ***Please share*** how this access benefits you. Your story matters.

Citation: Javid, Farhad et al. "Fatigue exhaustion of the mitral valve tissue." Biomechanics and Modeling in Mechanobiology 18, 1 (August 2018): 89–97 © 2018 Springer Nature

As Published: https://doi.org/10.1007/s10237-018-1070-3

Publisher: Springer Science and Business Media LLC

Persistent URL: https://hdl.handle.net/1721.1/128907

Version: Author's final manuscript: final author's manuscript post peer review, without publisher's formatting or copy editing

Massachusetts Institute of Technology

Noname manuscript No.
(will be inserted by the editor)

Fatigue Exhaustion of the Mitral Valve Tissue

Farhad Javid · Nastaran Shahmansouri · Jorge Angeles · Rosaire Mongrain

Received: date / Accepted: date

Abstract Sudden failure and rupture of the tissue is a rare but serious short-term complication after the mitral valve surgical repair. Excessive cyclic loading on the suture line of the repair can progressively damage the surrounding tissue and finally cause tissue rupture. Moreover, mechanical over-tension, which occurs in a diseased mitral valve, gradually leads to tissue floppiness, mitral annular dilation, and leaflet rupture. In this work, the rupture mechanics of mitral valve is studied by characterizing the fracture toughness exhaustion of healthy tissue. Results of this study show that fracture toughness of the posterior mitral valve is lower than its anterior counterpart, indicating that posterior tissue is more prone to failure. Moreover, the decrease of fracture toughness by increasing the number of fatigue cycles shows that excessive mechanical loading leads to progressive failure and rupture of mitral valve tissue within a damage accumulative process.

Farhad Javid
Koch Institute for Cancer Research, Massachussets Institute of Technology, 500 Main St., Cambridge, MA, 02140
Tel.: +1-617-710-6085
E-mail: farhad.javid@mail.mcgill.ca

Nastaran Shahmansouri · Jorge Angele · Rosaire Mongrain
Department of Mechanical Engineering, McGill University, 817 Sherbrooke St. W., Montreal, Quebec, H3A 0C3, Canada

Jorge Angeles
Centre for Intelligent Machines and Department of Mechanical Engineering, McGill University, 3480 University Street, Montreal, Quebec, H3A 2A7, Canada

Keywords Fracture toughness · Tissue rupture · Mitral valve · Suture failure · Percutaneous annuloplasty

1 Introduction

Mitral regurgitation (MR), backward leakage of blood from the left ventricle to the left atrium during systole, is a valvular heart disease with serious complications such as irreversible heart damage, cardiac arrhythmia, and heart failure. It is known that mechanical loading on the mitral valve (MV) tissue plays an important role in myxomatous degeneration, the most common cause of organic MR [1]. In addition, mitral annular dilation, the main geometric factor that contributes in functional MR [2–4], has a direct correlation with mechanical over-tension caused by dilated cardiomyopathy on the MV tissue [5,6]. However, the mechanism under which tissue deterioration and rupture are developed has not been investigated.

Progressive deterioration and rupture of MV tissue is also observed after mitral valve repair. In addition to the risks associated with open-heart surgery, rupture of the MV tissue around the suture line of a mitral annuloplasty[1] is a rare but serious complication that may occur shortly after the repair [7]. Tissue rupture leads to wound dehiscence, implant separation and, ultimately, to heart failure. Moreover, the rupture mechanics of the mitral valve tissue is very important in the design of self-anchoring fixation implants to replace standard suturing in percutaneous techniques, currently being developed to reduce the risk of annuloplasty [8–10]. Since such implants usually fail due to tissue tearing, the tissue resistance to rupture plays an important role in the design and optimization of new fixation implants.

In fracture mechanics, a material resistance to rupture is characterized by its fracture toughness. Also, the detrimental impact of repetitive forces on a material can be described by its fatigue behavior. Although these concepts have been exten-

[1] Mitral annuloplasty, the main repair technique of MR, consists of suturing a prosthetic ring to the annulus and shrinking the valve orifice to the normal or undersized dimensions.

sively used for studying failure in engineering and hard biological materials such as bone [11,12], there is a paucity of research on the fracture mechanics of soft tissue. Fracture toughness was first determined for *cooked* meat (muscle) due to its relevance to the food industry [13,14]. For living biological materials, the first study was reported on the skin tissue fracture toughness using a tearing test [15–17]. During the past three decades, similar studies were conducted on other types of soft tissue, such as cartilage [18], menisci [19], skin [15,17], liver [20,21], aorta [22–24], and muscle [25] . Studies on the fatigue behavior of soft biological materials are, however, limited only to connective tissue like cartilage [26,27], tendons [28], and ligaments [29].

In this paper, the fracture toughness of healthy MV tissue is characterized for the first time through a set of experiments. Moreover, the fatigue behavior of the tissue is studied by determining the effect of cyclic loading on its fracture toughness. In-house-developed devices are used to obtain fracture toughness and to apply cyclic loading to the tissue samples. Sample preparation, experimental procedures and setups of each test are explained in Section 2. The results are shown in Section 3 and a comprehensive discussion and conclusions are included in Sections 4 and 5.

2 Materials and methods

2.1 Materials

Fresh porcine hearts were obtained from a local slaughterhouse[2]. At the time of the slaughter, the animals were six months old and weighed 110–120 kg. The samples were randomly chosen from both male and female individuals. The effect of gender, thus, was not considered in this study. The MVs were meticulously dissected from the hearts, deep-frozen in liquid nitrogen and kept at -80° C prior to experiments. During freezing, the samples were submerged in a buffer solution

[2] Olymel Corp., Saint-Esprit, QC, Canada.

with 10% Dimethyl sulfoxide (DMSO) to minimize the damage to the extracellular matrix and preserve the mechanical properties of the tissue [30].

On the day of the experiments, the MVs were first thawed at room temperature and, then, cut to obtain rectangular strips of approximately 10×28 mm. The strips were excised from the top-mid section of each leaflet, including the MV annulus. The annulus is the section where a prosthetic ring is sutured to the MV in an annuloplasty repair; the rupture therefore occurs in this section. The length and the width of each sample were, respectively, parallel and perpendicular to the fiber direction in mitral leaflets. The MV structure with the fiber direction, the location of the tissue strips on both anterior and posterior leaflets, and the tissue samples are shown in Fig. 1. As can be seen, the posterior leaflets were not well-expanded and had many strut chords attached. The size and shape of the tissue strips obtained from the posterior leaflets were, therefore, unsuitable for the fatigue test setup. Fatigue effect was thus studied only on the anterior leaflet tissue, whereas fracture toughness on both anterior and posterior leaflets.

2.2 Fracture Toughness Characterization

Fracture toughness is defined as the energy required to generate a crack of unit area in a material. To find fracture toughness, a controlled crack is induced in the material sample, then, the energy required for this process is measured. The crack may be generated under: a normal tensile loading perpendicular to the crack face (mode-I); in-plane shear loading parallel to the crack face and perpendicular to the crack front (mode-II); or out-of-plane shear loading parallel to the crack face and parallel to the crack front (mode-III). Mode-I is known as the most critical type of crack with the lowest value of fracture toughness and the highest value of stress intensity factor at the crack tip.

Fracture toughness can be measured using a variety of destructive techniques including tearing [31], scissoring [32], and assorted guillotine cutting[3] [33,34]. Tearing test characterizes mode-I fracture toughness if an in-plane normal tension is applied to the sample. If an out-of-plane tension is applied, this technique is called trouser tear test and characterizes mode-III fracture toughness. Scissoring mixes modes I and III since cutting happens due to both the wedging effect and the out-of-plane motion of the blades. Guillotine test mainly determines mode-I fracture toughness due to the wedging effect of the blade in the crack propagation stage. The crack initiation, however, occurs mostly in mode-II. A lubricated cutting test (guillotine) was selected to obtain the mode-I fracture toughness of the MV tissue [35,23]. As shown in Fig. 2a, a razor blade is first passed through the tissue sample to make a length-controlled crack. A Sensotec Model 31 miniature 1-kg load cell (Honeywell, Columbus, USA) is mounted behind the tissue holder to measure the tissue reaction force during the process. Although oil lubrication is used, the force measured during the cutting process consists of both the friction between the tissue and the blade, and the fracture force required to propagate the crack. The friction force, however, can be evaluated in a second cycle by passing the blade through the cut sample. The fracture force can be found as

$$F_{\text{fracture}} = F_{\text{cutting}} - F_{\text{friction}} \tag{1}$$

where F_{cutting} is the cutting force measured during the first cycle, F_{friction} the friction force measured during the second cycle, and F_{fracture} the actual fracture force required to induce the crack. The fracture work is readily obtained as the integral of the fracture force over the cutting length as

$$W_{\text{fracture}} = \int_L (F_{\text{cutting}} - F_{\text{friction}}) \mathrm{d}s \tag{2}$$

[3] Needle insertion can also be considered as a practical technique for measuring fracture toughness in soft biological tissue [21]

where s is the arc-length variable along the crack and L the total length of the crack induced by the blade. Fracture toughness J is finally calculated as,

$$J = \frac{W_{\text{fracture}}}{A_{\text{fracture}}} \tag{3}$$

where A_{fracture} is the area of the two cut surfaces.

It should be mentioned that the slice-push technique, introduced by [36], is used to minimize the initial indentation energy. As can be seen in Fig. 2, the blade cuts the tissue at an inclined angle to minimize the perpendicular indentation forces applied to the sample. The slice-push ratio is defined as the ratio of the sideways horizontal (slicing) motion m of the blade to its vertical cutting motion p. A slice-push ratio of $3.5 : 1$ was chosen in the design of the fracture device.

The custom-designed fracture toughness device used in this study is shown in Fig. 2b. The device consists of a) a lever assembly on which the razor blade is attached and b) a sample-holding section. The lever assembly magnifies the device input motion four times and gives the blade adequate vertical motion to cut the samples. A load cell is used between the sample holder and the device base to measure the forces applied to the tissue during the experiments. To conduct the experiments, the device is mounted on the ELF 3200 platform to apply the input motion and to measure the output load cell forces.

The tissue samples were glued to the sample holder and mounted on the device load cell. In each test, the razor blade was passed through the tissue twice to measure both the cutting and the friction forces. The thickness of each sample was measured using a digital caliper in four points along the cut line and averaged to find the crack area.

2.3 Fatigue Assessment

To study fatigue, a total of 16 tissue strips with proper size and thickness for fatigue tests were obtained from the anterior leaflets of the porcine MVs. These

samples were divided into four fatigue groups of four and subjected to 10^3, 10^4, 10^5, and 10^6 tensile fatigue cycles, respectively. A sinusoidal tensile strain of 15% at a frequency of 15 Hz was applied along the fiber direction of the tissue strips. Considering the size, each sample underwent displacement-controlled tension of $d = 2.1\sin(30\pi t)$ mm in each cycle. The strain applied to the samples during the fatigue test was slightly higher than the normal strain values applied to healthy MV tissue in a beating heart. Real-time *ex-vivo* measurements have shown that the largest strains are exerted on the belly region of the anterior leaflet of a healthy heart with peak values of 7.8% and 5.0% along the circumferential and radial directions, respectively [37]. A similar study on the MV after a controlled myocardial infarction showed that the strain values could be up to 25–30% [5]. Conversely, although the local strain in the tissue-implant anchoring zone is not readily known, it is expected to be much higher than the above-mentioned values for the healthy and the diseased MV. Higher values of strain may lead to faster and more severe damage to the tissue. To account for the effect of high strain values in both diseased and repaired hearts, a slightly above-normal strain of 15% was applied along the fiber direction of the tissue strips. On the other hand, the fatigue tests were conducted at 15 Hz to shorten the test duration and to prevent the biological degradation of the tissue. The ideal frequency for the tests is the average cardiac rhythm, 1.2 Hz [38]. However, applying 1M load cycles at this frequency takes more than 10 days.

Fatigue tests were conducted by utilizing an in-house-designed device [23]. As shown in Fig. 3, the fatigue device consists of a sliding and a fixed arm placed in a water bath. The device is mounted on a Bose EnduraTech ELF 3200 (Bose Corporation, Framingham, USA) platform while its sliding arm is connected to ELF 3200 Axis 1 to apply periodic loading on the tissue samples.

As shown in Fig. 3a, the tissue strips obtained from the anterior MV leaflets were glued to a pair of mounting racks using commercial cyanoacrylate glue (Gorilla Glue Inc, Cincinnati,USA). A special jig was used to keep the racks parallel

at 14 mm apart while gluing the samples. The tissue racks were then pinned on the device arms to undergo fatigue loading. The temperature of the samples was controlled at $37 \pm 1^{\circ}$C during the tests. To minimize proteolytic degradation, the samples were tested within one hour of being thawed. Also, the tissue strips were submerged in a buffer solution during the course of the experiments.

3 Results

3.1 Intact Tissue

To characterize the fracture toughness of the healthy MV tissue, a set of four samples was excised from both the posterior and the anterior MV leaflets and tested by the custom-made fracture toughness device. One anterior sample was excluded from the results since the tissue was extremely thin (< 0.5 mm) and it did not show a stable region in the force-displacement curve. Figure 4 shows a generic force-displacement curve obtained during the guillotine test on an anterior and a posterior tissue sample. Each graph contains two loops, the first obtained during the cutting cycle, the second during the friction cycle. The returning curves, describing the blade moves backward to leave the tissue, are also shown. The area between the force-displacement cutting and friction cycles provides the fracture energy of the tissue. To reduce the fraction of mode-III fracture in the results, only the steady state section of the cycles, highlighted in Fig. 4, are used for calculations [22]. The fracture toughness value is obtained by dividing the fracture energy, the area between the two curves in the steady interval, by the cutting area of this section. Details of the fracture tests are displayed in Table 1. The average toughness value of the anterior and the posterior MV tissue are, respectively, 137.35 and 66.27J/m^2.

3.2 Fatigued Tissue

Results of the guillotine tests on the anterior leaflets are displayed in Table[4] 2. It should be mentioned that one test in the 10^6-cycle fatigue group failed and was excluded from the results, since the blade contacted the tissue holder during the test. Fracture toughness of the anterior MV tissue is plotted in Fig. 5 versus the number of fatigue cycles. Power-law functions are commonly used to describe the material behavior under fatigue. As shown in Fig. 5, a power-law function is fitted to the decreasing trend of fracture toughness (correlation coefficient $R^2 = 0.86$).

4 Discussion

The main objective of this paper is to characterize the fracture toughness of the MV tissue and to evaluate its progressive degradation under load cycles. The fracture toughness of both the anterior and the posterior MV leaflets was characterized here. The results show that fracture toughness in the anterior mitral leaflet is higher than twice that of its posterior counterpart. This is consistent with the posterior leaflet being more prone to degenerative disorders, such as mitral leaflet prolapse and leaflet rupture, as compared to the anterior one [39]. Moreover, the progressive deterioration of the anterior mitral leaflet was studied by the short-term fatigue effect of mechanical loading on the fracture toughness properties of the tissue. A maximum reduction of 25% was observed in the mean values of the fracture toughness after one million fatigue cycles.

The fracture toughness of a material mainly characterizes its resistance to crack propagation and rupture. As mentioned in Section 1, tissue rupture could occur on the suture lines in a repaired MV shortly after the operation. Characterizing fracture toughness and its short-time evolution under cyclic loading is, therefore, a useful property in the design and optimization of new surgical fasteners for percutaneous repair techniques. Knowing fracture toughness, we can predict tissue

[4] The results of the control group, not subjected to fatigue loading, can be found in Table 1.

failure in the tissue-implant interaction zone. The results of this model can thus be used to maximize the anchoring performance of new surgical implants. This is the subject of a future work.

The fracture toughness of the MV tissue was characterized in this study for the first time; therefore, there are no experimental data in the literature. Fracture toughness of similar tissue types, however, has been studied. For example, fracture toughness of swine and human ascending aorta has been measured as 290 and 100 J/m^2, respectively, using a similar guillotine test [23,24]. Fracture toughness of swine liver has been quantified as 76–185 J/m^2 using needle insertion [21], and as 187–225 J/m^2 using a scalpel cutting tool [20]. Moreover, the fracture toughness of a variety of mammalian soft tissue was determined [17] using a scissor-cutting technique, and the fracture resistance of a cultured neocartilage was characterized [40]. The fracture toughness values obtained in this work are in the range of the values measured in the aforementioned studies.

The decreasing trends observed in fracture toughness values represent the effect of induced fatigue on the mechanical properties of the MV tissue. In similar studies, the effect of fatigue on the fracture toughness and elastic properties of porcine coronary and aortic tissue has been reported [23, 41]. Based on Lemaître's theory, the fatigue effect on fracture toughness and elastic modulus is governed by a damage accumulation process in the material [42]. Power-law functions are, therefore, fitted to the mean value of the fracture toughness versus the number N of fatigue cycles as

$$J_N = J_0 N^{\beta} + J_1, \tag{4}$$

where subscript N in J_N is used to refer to the value of J after N fatigue cycles and J_0, J_1 and β are the curve constants shown in Fig. 5. Knowing the effect of fatigue on the elastic properties of the tissue [23], equation (4) could be used to directly relate fracture toughness to elastic modulus. This is important, since fracture toughness is characterized through destructive measurement techniques that are not applicable in clinical cases. However, the elastic properties can be

found through existing non-destructive clinical methods. Knowing this relation, the fracture toughness can be indirectly calculated through noninvasive clinical testing.

It has been shown that pathological changes in the mechanical loading on the mitral valve lead to microstructural alteration in the tissue [43–47] and changes its mechanical properties [48–52]. Similarly, cyclic loading causes collagen-fiber reorientation, while changing the extracellular matrix of the tissue. Such fatigue effects are also observed in bioprosthetic heart valves (BHVs) [53,54], which are made of chemically modified, hence, nonviable collagenous soft tissue. The cyclic mechanical loading on BHVs leads to fiber reorientation, matrix alteration and, eventually, to mechanical failure of the tissue [55–57].

In-vivo measurements have shown substantial residual strains in the mitral valve tissue [58], which may affect the fatigue failure of the tissue under cyclic loading. For regular engineering materials such as metals, Paris' law relates the crack growth and fatigue life to the variation of the stress intensity factor in each load cycle [59]. However, a mean stress can affect the fatigue life while the alternating stress is fixed [60]. The effect of the mean stress can be predicted by the Goodman diagram of failure for engineering materials. In general, the mean stress decreases fatigue life since it leads to higher absolute values of stress in the material in each cycle. For viable biological materials, however, the conditions may be more complicated since tissue can adjust itself to the new conditions.

4.1 Limitations

Considering the morphology of the MV leaflets, it was not feasible to obtain more than one sample from each leaflet. The variations of the mechanical properties among samples of different individuals were, therefore, not considered in this study. Nevertheless, in order to reduce the effect of these variations, a group of four samples was tested; the mean value of each group was used for further evaluation.

The samples were tested *in-vitro*, where the effect of mechanical factors takes over the effect of biological parameters. The latter can potentially heal the progressive damages by cellular and enzymatic activities in living tissue. This effect, however, is not dominant in the low cycle fatigue (1 million cycles) considered here. Moreover, the mechanical properties of biological tissue are largely determined by the extracellular matrices, which do not change rapidly by biological activities and remain almost intact during *in-vitro* experiments.

Finally, the existence of the cords in the tissue samples can significantly affect the results of the experiments and increase the variations among them. Hence, special care was applied to prepare smooth and uniform tissue samples.

5 Conclusions

To the best of the authors knowledge, the fracture toughness of both the anterior and the posterior MV leaflets has been characterized for the first time, therefore there are no experimental data in the literature. The results have shown that fracture toughness in the anterior leaflet is higher than that of its posterior counterpart. The progressive deterioration of the MV tissue has been also studied by characterizing the fatigue effect on the fracture toughness of the tissue. The fracture toughness of the tissue shows a decreasing trend under periodic mechanical loading.

The results of this study help to better understand the tissue failure process in the suturing area of a repaired MV. Th value of the fracture toughness can be used as the ultimate failure criterion of the MV tissue. Also, the evolution of fracture toughness reveals that mechanical changes may occur in degenerative MV diseases as a result of excessive mechanical loading on the tissue. Hence, the fracture toughness of the MV tissue is one of the main factors in the design of the new fixation implants that maximize their anchoring forces without tearing the tissue.

Conflict of interest statement

There is no conflict of interest for any author related to this article.

Acknowledgements

We wish to thank Mr. Boby Chu for the design and fabrication of the fatigue and the fracture toughness devices and Dr. Amir K. Miri Ramsheh for helping us to set up and to calibrate the devices. We also thank NSERC, Canada's Natural Sciences and Engineering Research Council, and FRQNT, Quebec's Fonds de recherche du Québec Nature et Technologies, for their financial support.

References

1. L. Pedersen, J. Zhao, J. Yang, P. Thomsen, H. Gregersen, J. Hasenkam, M. Smerup, H. Pedersen, L. Olsen, Research in Veterinary Science **82**(2), 232 (2007)
2. E. Agricola, M. Oppizzi, F. Maisano, M. De Bonis, A.F. Schinkel, L. Torracca, A. Margonato, G. Melisurgo, O. Alfieri, Circulation **5**, 326 (2004)
3. B.H. Trichon, C.M. O'Connor, American Heart Journal **144**(3), 373 (2002)
4. A.C. Hueb, F.B. Jatene, L.F.P. Moreira, P.M. Pomerantzeff, E. Kallás, S.A. De Oliveira, Journal of Thoracic and Cardiovascular Surgery **124**, 1216 (2002)
5. M.K. Rausch, F.A. Tibayan, N.B. Ingels, D.C. Miller, E. Kuhl, Annals of Biomedical Engineering **41**(10), 2171 (2013)
6. M. Padala, R.A. Hutchison, L.R. Croft, J.H. Jimenez, R.C. Gorman, J.H.G.J. III, M.S. Sacks, A.P. Yoganathan, The Annals of Thoracic Surgery **88**(5), 1499 (2009)
7. M. De Bonis, F. Maisano, G. La Canna, O. Alfieri, Nature Reviews Cardiology **9**, 133 (2012)
8. V. Rudolph, S. Baldus, Herz **38**, 136 (2013)
9. R.S. Schofield, P.M. Schofield, Journal of the Saudi Heart Association **22**, 111 (2010)
10. F. Tops, S. Kapadia, E. Tuzcu, A. Vahanian, O. Alfieri, J. Webb, J. Bax, Current Problems in Cardiology **33**(8), 417 (2008)
11. D. Taylor, J. Hazenberg, T. Lee, Journal of Theoretical Biology **225**(1), 65 (2003)
12. O.C. Yeh, T.M. Keaveny, Journal of Orthopaedic Research **19**(6), 1001 (2001)
13. A.S. Szczesniak, K.W. Torgeson, Advances in Food Research **14**, 33 (1965)
14. P.P. Purslow, Meat Science **12**(1), 39 (1985)

15. P. Purslow, Journal of Materials Science **18**(12), 3591 (1983)
16. R. Cohen, M. Zimber, J. Hansbrough, Y. Fung, J. Debes, R. Skalak, in Annals of Biomedical Engineering, ed. by J. Lee (1991), pp. 600–601. Pergamon, NY
17. B. Pereira, P. Lucas, T. Swee-Hin, Journal of Biomechanics **30**(1), 91 (1997)
18. M.V. Chin-Purcell, J.L. Lewis, Journal of Biomechanical Engineering **118**, 545556 (1996)
19. M. Sonoda, F.L. Harwood, M.E. Amiel, H. Moriya, M. Temple, D.G. Chang, L.M. Lottman, R.L. Sah, D. Amiel, The American Journal of Sports Medicine **28**(1), 90 (2000)
20. T. Chanthasopeephan, J. Desai, A. Lau, in Biomedical Robotics and Biomechatronics, 2006. BioRob 2006. The First IEEE/RAS-EMBS International Conference on (2006), pp. 899–904
21. T. Azar, V. Hayward, in Biomedical Simulation, Lecture Notes in Computer Science, vol. 5104 (2008), pp. 166–175
22. P.P. Purslow, Journal of Biomechanics **16**(11), 947 (1983)
23. B. Chu, E. Gaillard, R. Mongrain, S. Reiter, J.K. Tardif, Journal of the Mechanical Behavior of Biomedical Materials **17**, 126 (2012)
24. N. Shahmansouri, M. Alreshidan, A. Emmott, K. Lachapelle, R. Cartier, R.L. Leask, R. Mongrain, Journal of the mechanical behavior of biomedical materials **64**, 262 (2016)
25. D. Taylor, N. OMara, E. Ryan, M. Takaza, C. Simms, Journal of the Mechanical Behavior of Biomedical Materials **6**(0), 139 (2012)
26. T. McCormack, J.M. Mansour, Journal of Biomechanics **31**(1), 55 (1997)
27. G. Bellucci, B.B. Seedhom, Biorheology **39**(1-2), 193 (2002)
28. H. Schechtman, D. Bader, Journal of Biomechanics **30**(8), 829 (1997)
29. R.G. Pollock, V.M. Wang, J.S. Bucchieri, N.P. Cohen, C.Y. Huang, R.J. Pawluk, E.L. Flatow, L.U. Bigliani, V.C. Mow, Journal of Shoulder and Elbow Surgery **9**(5), 427 (2000)
30. M.J. Chow, Y. Zhang, Journal of Surgical Research **171**(2), 434 (2011)
31. G. Lake, Rubber Chemistry and Technology **76**(3), 567 (2003)
32. C. McCarthy, M. Hussey, M. Gilchrist, Engineering Fracture Mechanics **74**(14), 2205 (2007)
33. A. Atkins, Y. Mai, Journal of Materials Science **14**(11), 2747 (1979)
34. B. Darvell, P. Lee, T. Yuen, P. Lucas, Measurement Science and Technology **7**(6), 954 (1996)
35. N. Shahmansouri, R. Cartier, R. Mongrain, Journal of Biomechanics **48**(10), 2205 (2015)
36. A. Atkins, X. Xu, G. Jeronimidis, Journal of Materials Science **39**(8), 2761 (2004)
37. M.K. Rausch, W. Bothe, J.E.K. Vitting, J.C. Swanson, N.B. Ingels, D.C. Miller, E. Kuhl, Annals of Biomedical Engineering **39**(6), 1690 (2011)
38. W. Boron, E. Boulpaen, Medical physiology: a cellular and molecular approach (Elsevier Saunders, Philadelphia, 2005)

39. O. Alfieri, M. De Bonis, Interventional Cardiology (London) **7**(2), 131 (2012)
40. M. Oyen-Tiesma, R. Cook, Journal of Materials Science: Materials in Medicine **12**(4), 327 (2001)
41. C. Gilpin, Cyclic loading of porcine coronary arteries. Master's Thesis, Georgia Institute of Technology, Atlanta (2005)
42. J. Lemaître, A course on damage mechanics (Springer-Verlag, Berlin, Germany, 1996)
43. Y.C. Fung, S.Q. Liu, Journal of Applied Physiology **70**(6), 2455 (1991)
44. J. Liao, L. Yang, J. Grashow, M. Sacks, Journal of biomechanical engineering **129**, 78 (2007)
45. K.S. Kunzelman, D.W. Quick, R.P. Cochran, The Annals of Thoracic Surgery **66**(6), S198 (1998)
46. D.W. Quick, K.S. Kunzelman, J.M. Kneebone, R.P. Cochran, ASAIO journal (American Society for Artificial Internal Organs: 1992) **43**(3), 181 (1997)
47. B.V. Rego, S.M. Wells, C.H. Lee, M.S. Sacks, Journal of The Royal Society Interface **13**(125) (2016)
48. K.S. Kunzelman, R.P. Cochran, Journal of Cardiac Surgery **7**(1), 71 (1992)
49. K. May-Newman, F.C. Yin, Journal of Biomechanical Engineering **120**(1), 38 (1998)
50. V. Prot, B. Skallerud, G.A. Holzapfel, International Journal for Numerical Methods in Engineering **71**, 987 (2007)
51. C.H. Lee, J.P. Rabbah, A.P. Yoganathan, R.C. Gorman, J.H. Gorman, M.S. Sacks, Biomechanics and Modeling in Mechanobiology **14**(6), 1281 (2015)
52. W. Zhang, S. Ayoub, J. Liao, M.S. Sacks, Acta Biomaterialia **32**, 238 (2016)
53. W. Sun, M. Sacks, G. Fulchiero, J. Lovekamp, N. Vyavahare, M. Scott, Journal of Biomedical Materials Research Part A **69A**(4), 658 (2004)
54. T.L. Sellaro, D. Hildebrand, Q. Lu, N. Vyavahare, M. Scott, M.S. Sacks, Journal of Biomedical Materials Research Part A **80A**(1), 194 (2007)
55. W. Zhang, M.S. Sacks, Journal of the Mechanical Behavior of Biomedical Materials **75**, 336 (2017)
56. S.M. Wells, T. Sellaro, M.S. Sacks, Biomaterials **26**(15), 2611 (2005)
57. S.M. Wells, M.S. Sacks, Biomaterials **23**(11), 2389 (2002)
58. R. Amini, C.E. Eckert, K. Koomalsingh, J. McGarvey, M. Minakawa, J.H. Gorman, R.C. Gorman, M.S. Sacks, Annals of Biomedical Engineering **40**(7), 1455 (2012)
59. P.C. Paris, M.P. Gomez, W.E. Anderson, The trend in engineering **13**(1), 9 (1961)
60. J. Yuen, J. Copeland, Journal of Engineering Materials and Technology **101**(3), 214 (1979)

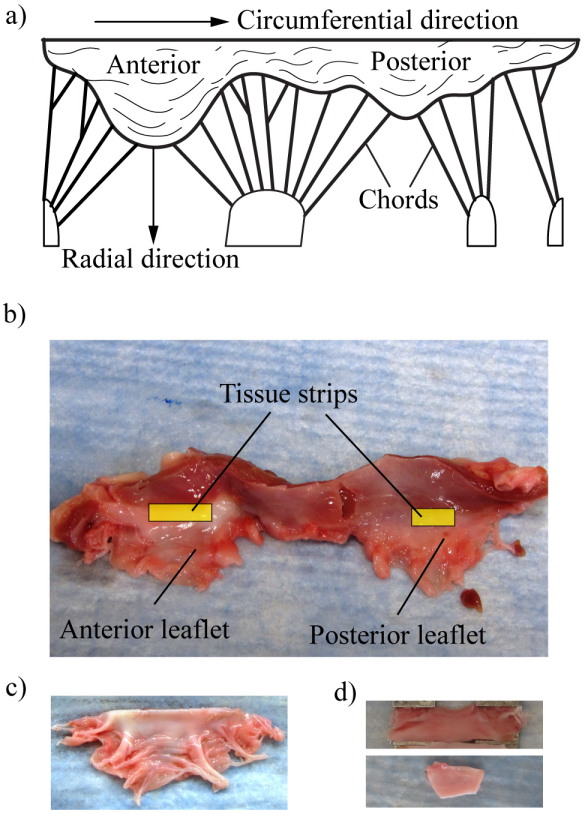

Fig. 1 Mitral valve structure: a) A schematic illustration of MV with fibers, b) MV structure and the location of tissue strips, c) morphology of the posterior leaflet, and d) tissue samples obtained for fatigue (top) and fracture toughness (bottom).

a)

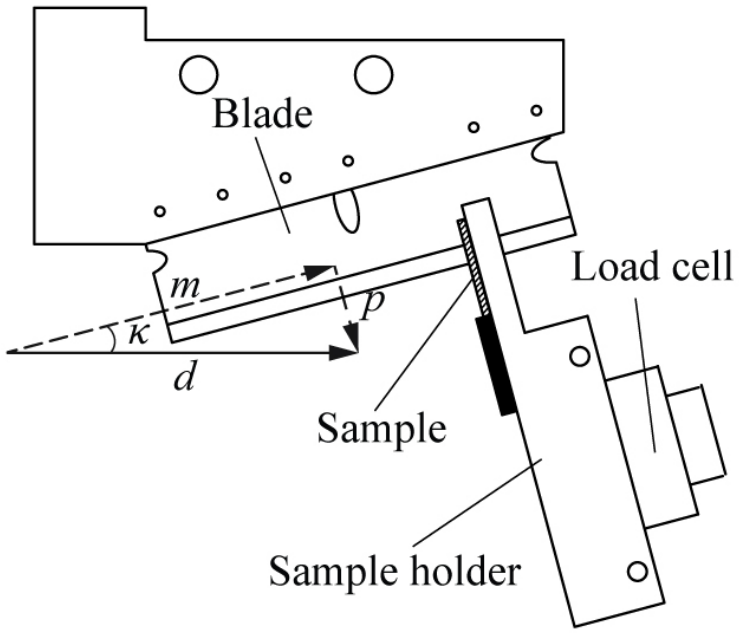

b)

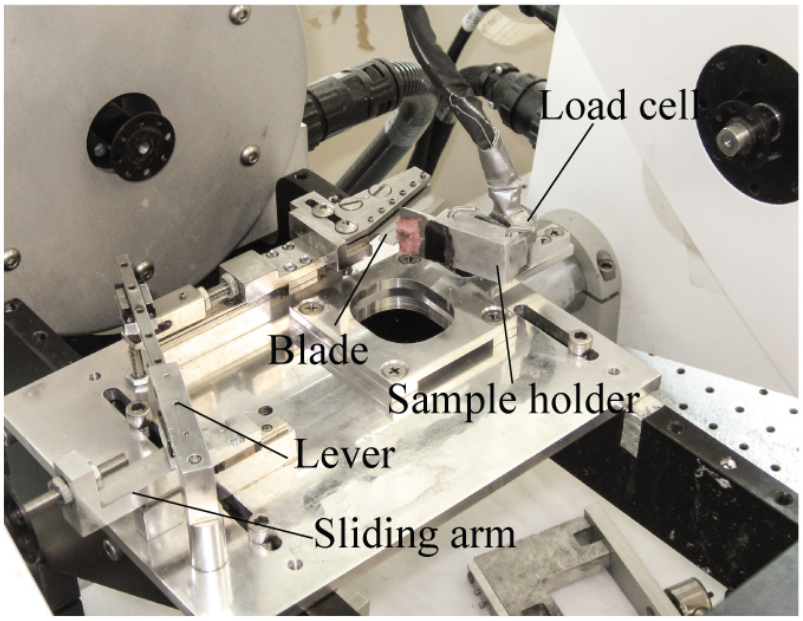

Fig. 2 a) A sketch of the guillotine test conducted to measure fracture toughness, b) the custom-made fracture toughness device.

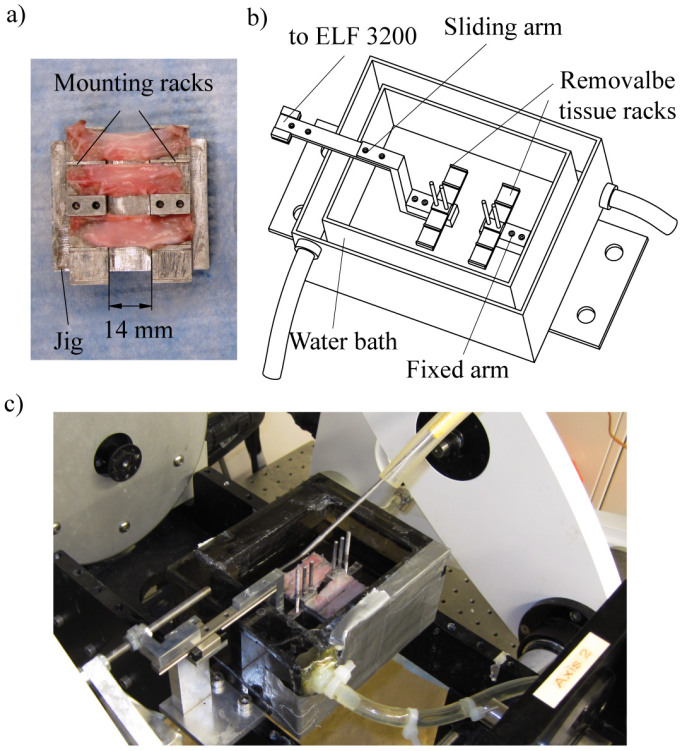

Fig. 3 a) Tissue strips glued to a pair of mounting racks kept 14 mm apart by a special jig, b) a sketch of the fatigue test apparatus, and c) the custom-made fatigue device.

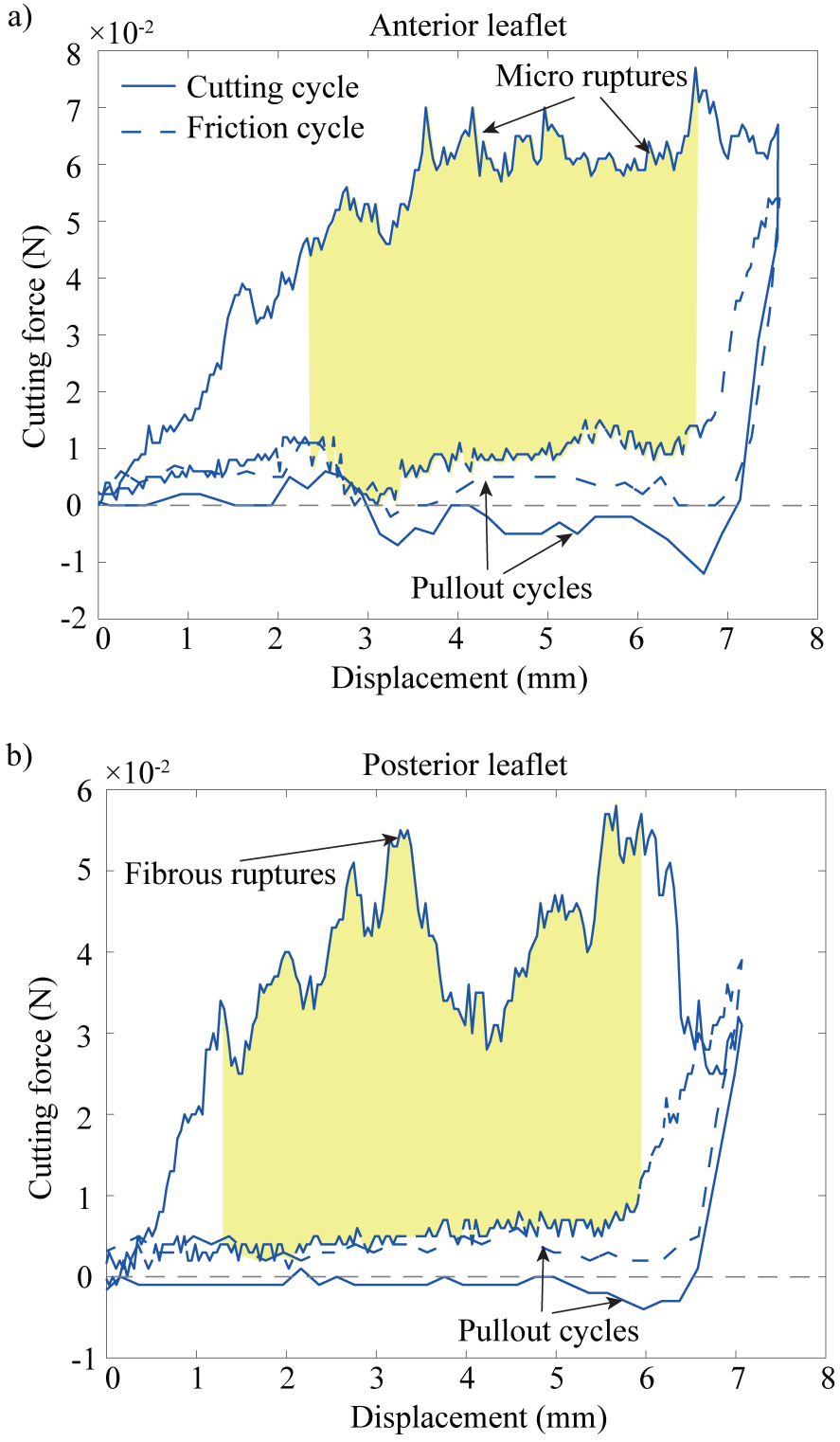

Fig. 4 Force-displacement curves in the cutting and the friction cycles for a) anterior and b) posterior leaflet samples.

Table 1 Fracture toughness of the posterior mitral leaflet

Tissue samples	Thickness (mm)	Area (mm^2)	$W_{fracture}$ ($\times 10^{-6}$J)	J (J/m^2)	
				Tests	Avg. ±SD
Anterior	0.67	5.98	793.81	132.73	137.35 ±26.73
	0.98	4.72	784.91	166.08	
	0.71	8.24	932.56	113.23	
Posterior	0.90	9.16	611.58	66.70	66.27 ±5.87
	1.54	10.80	796.20	73.73	
	1.02	5.34	317.06	59.48	
	0.90	9.58	624.59	65.19	

Table 2 Fracture toughness of the anterior mitral leaflet versus fatigue

Fatigue cycles	Thickness (mm)	Area (mm^2)	$W_{fracture}$ ($\times 10^{-6}$J)	J (J/m^2)	
				Tests	Avg. ±SD
1000	0.77	7.62	764.08	100.36	134.74 ±37.84
	0.72	4.60	699.67	151.84	
	0.58	3.86	692.87	179.91	
	1.25	9.50	1014.78	106.82	
10,000	0.93	7.44	1009.05	135.63	121.63 ±12.74
	0.85	7.46	917.03	122.93	
	0.62	6.60	690.46	104.73	
	0.78	6.20	764.18	123.26	
100,000	0.61	4.46	358.30	80.46	110.96 ±35.73
	0.81	6.64	924.92	139.26	
	0.52	6.28	477.71	79.69	
	0.58	5.06	713.12	144.45	
1,000,000	0.51	3.88	320.2	82.46	111.73 ±25.81
	0.72	4.52	596.61	131.94	
	0.88	4.80	577.73	120.60	

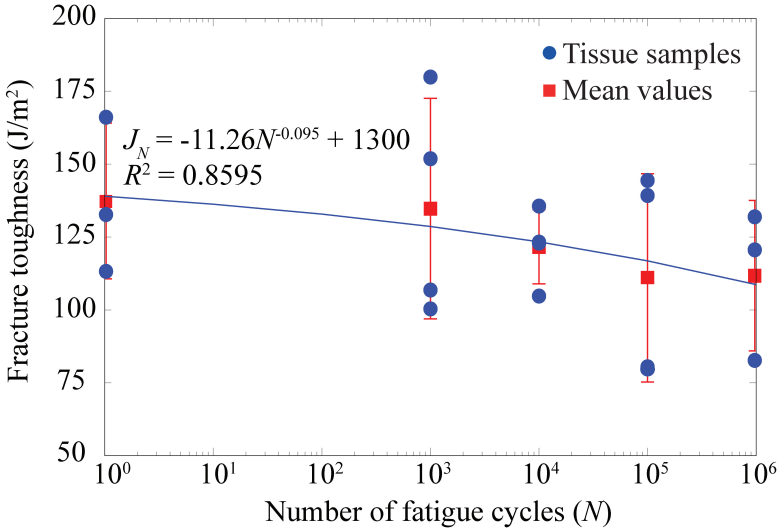

Fig. 5 Evolution of fracture toughness in the anterior MV leaflets versus number of fatigue cycles